Available online at www.sciencedirect.com
SCIENCE DIRECT®
Journal of Colloid and Interface Science 274 (2004) 294–308
JOURNAL OF Colloid and Interface Science
www.elsevier.com/locate/jcis

Instability of the interface between thin fluid films subjected to electric fields

V. Shankar * and Ashutosh Sharma

Department of Chemical Engineering, Indian Institute of Technology, Kanpur 208016, India

Received 7 August 2003; accepted 10 December 2003

Abstract

The effect of an externally applied electric field on the stability of the interface between two thin leaky dielectric fluid films of thickness ratio β and viscosity ratio μ_r is analyzed using a linear stability analysis in the long-wave limit. A systematic asymptotic expansion is employed in this limit to derive the coupled nonlinear differential equations describing the evolution of the position of the interface between the fluids and the interfacial free charge distribution. The linearized stability of these equations is determined and the effect of the ratio of the conductivities, dielectric constants, thicknesses, and viscosities on the wavenumber of the fastest growing mode, $k_{\max}$, and the growth rate of the most unstable mode, $s_{\max}$, is examined in detail. Specific configurations considered in previous studies, such as a perfect dielectric–air interface, leaky dielectric–air interface, etc., emerge as limiting cases from the general formulation developed in this paper. Our results show that the viscosity ratio, μ_r, does not have any significant effect on $k_{\max}$ for the interface between perfect and leaky dielectric fluids. In marked contrast, however, μ_r is shown to have a significant effect on the interface between two leaky dielectrics. Increasing μ_r from 0.1 to 10 could decrease $k_{\max}$ up to a factor of 5. In general, our results show that the presence of nonzero conductivity in either one or both of the fluids has a profound influence on the length-scale characteristic of the linear instability: a reduction even by a factor of $1/50$ in the length scale can be effected when compared to the interface between two perfect dielectrics. These predictions could have important implications in pattern formation applications in thin fluid films that employ electric fields. The variation of $k_{\max}$ and $s_{\max}$ on the thickness ratio, β, indicates in general that $k_{\max} \propto \beta^{-\alpha}$, and $s_{\max} \propto \beta^{-\theta}$, where the exponents α and θ (both > 0) are found to depend only on the ratio of conductivities, and are largely independent of other system parameters.

Keywords: Leaky dielectric film; Linear stability analysis; Long-wave approximation; Electric field; Dielectric fluids

1. Introduction

The effect of electric fields on the stability and dynamics of fluid–fluid interfaces has been an area of extensive research, beginning from the classic works of Taylor and McEwan [1] and Melcher and Smith [2]. These works and subsequent studies (see, for example, the review of Saville [3]) have amply demonstrated the role of electrical stresses on fluid interfaces, and the associated electrohydrodynamic instabilities in such systems. One of the basic problems here is to understand the stability of the interface between two fluid layers bounded on the top and bottom by rigid plates, and this has been the subject of many previous studies. These studies have largely considered systems in which gravitational effects are important, and therefore a critical applied voltage is required to cause the instability: very long waves are stabilized by gravity, and short waves are stabilized by interfacial tension, and waves of intermediate lengths become unstable. These earlier studies have focused on how the critical voltage required for instability is affected by the nature of the fluids, viz. whether they are perfect dielectrics, or whether they are "leaky" dielectrics [3] in which there is the possibility of free charge conduction in the fluids, and also the possibility of accumulation and redistribution of charges on the interface between two fluids. Recently, there has been a renewed interest in this area, in part due to the relevance of such phenomena in the formation of well-controlled patterns using the application of electric fields to thin liquid films. For example, Russel, Steiner, and co-workers have demonstrated [4–8] that the application of an external electric field to polymer–air or polymer–polymer interfaces enhances the spontaneous fluctuations at the in-

* Corresponding author.
E-mail addresses: vshankar@iitk.ac.in (V. Shankar), ashutos@iitk.ac.in (A. Sharma).

0021-9797/$ – see front matter
doi:10.1016/j.jcis.2003.12.024

terface leading to an instability and the formation of well-defined columnar structures. In the polymer–air case [4], if the upper surface is patterned, say in the form of columns, the instability at the interface replicates the lateral pattern. Observations similar to these authors were also made by Chou and co-workers [9,10], even in the absence of electric fields. In their experiments, electric fields were generated naturally from the contact potentials of the different interfaces (also see [11]).

An important difference between these recent experimental studies and the earlier studies is that these experiments were performed in systems where the thicknesses of liquid films were about 100 to 1000 nm, and at such length scales, gravity is not expected to be dominant. Thus, the interfaces between these thin films exhibit a long-wave instability under the application of electric fields, in contrast to the case when gravity is dominant where waves of finite lengths become unstable. Thus, the length scale that dominates the linear instability in the long-wave instability is the wavelength of the fastest growing mode. The signature of this length scale is also seen in the ordered patterns that are formed as a result of the nonlinear evolution processes that occur after the linear instability. Therefore, the issue of importance in these experiments is not the threshold voltage and the critical wavelength, but the wavelength of the fastest growing mode.

Recent theoretical studies [5,6,11,12] that have considered the linear stability characteristics of thin fluid films subjected to electric fields were restricted to the following configurations: (1) the interface between a perfect dielectric liquid and air [5], (2) the interface between two perfect dielectric liquids [6], (3) the interface between a dielectric fluid of finite thickness and a conducting fluid of much larger thickness [11], and (4) the interface between a leaky dielectric liquid and air [12].

Except the study of Pease and Russel [12], all these studies have focused only on perfect dielectric systems. The presence of conductivity in one or both of the liquids could have a significant impact on the length scales and growth rates, and this has been noted in [12]. This is especially attractive from the viewpoint of pattern formation techniques requiring semiconducting or conducting polymers with conjugated double bonds or doped polymers in optoelectronic applications. Conductivity also can be very high if aqueous films are used. In this study, we consider the most general case of the interface between two leaky dielectric fluids with arbitrary viscosities and conductivities, and analyze the linear stability characteristics in the long-wave limit. The specific configurations considered in previous studies emerge as special limiting cases from our general formulation. We first use a systematic long-wave asymptotic analysis and derive the nonlinear evolution equations for the interface position and interfacial charge distribution, and we subsequently study the linearized stability of the nonlinear differential equations. In the remainder of this Introduction, relevant previous studies are briefly summarized, and the context and motivation for the present work is placed in perspective.

The early study of Melcher and Smith [2] has considered the linear stability of two conducting viscous fluids while including the dynamics of the surface charge. In their work, gravity plays an important role, and stabilizes the long waves, thus giving rise to a critical finite wavelength that becomes unstable at a threshold voltage. They have considered several special cases, such as perfectly conducting and perfectly insulating interfaces, and concluded that even a slight amount of surface charge makes the interface unstable at a considerably lower voltage than would be expected from theories based on perfectly dielectric fluids with no interfacial free charge. While the present work shares some similarities with [2] in the formulation of the governing equations, we consider length scales in which gravity is unimportant, and so the results of the present analysis differ markedly from [2]. More recently, Schaffer et al. [5] have considered the case of a polymer–air interface, where the polymer is modeled as a perfect dielectric. They used a long-wave analysis to calculate the wavelength of the fastest growing mode, $\lambda_{\max}$, and how this is affected by the electric field, surface tension, and dielectric constants. Their theoretical predictions for $\lambda_{\max}$ as a function of the electric field in the fluid were shown to be in good agreement with their experimental observations.

Subsequently, Lin et al. [6] carried out both theory and experiments on polymer–polymer interfaces to study the variation of $\lambda_{\max}$ with the viscosity ratio, μ_r, between the two fluids and other parameters noted above. Both polymers were modeled as perfect dielectrics. Their theoretical results showed that $\lambda_{\max}$ is independent of μ_r, and in general there was a qualitative agreement between their predictions and experimental observations for $\lambda_{\max}$. However, they concluded that the experimentally inferred growth rate was very large (by a factor of 50) for the polymer–polymer case when compared to the polymer–air case, while the theory predicts nearly the same growth rates for both these systems. Lin et al. [7] followed up their previous work by an extensive experimental study which used a variety of polymers, and they concluded that the theoretical predictions for $\lambda_{\max}$ was in good agreement with their observations. They further noted that the discrepancy in the growth rates between theory and observations could be due to the inability to characterize the early stage kinetics of the growth quantitatively. Herminghaus [11] has considered the interface between a dielectric fluid of finite thickness, h_0, and a conducting fluid of much larger thickness. This analysis included van der Waals forces and showed that the wavenumber of the fastest growing mode decreases as $h_0^{-3/2}$, when the dispersion forces are not dominant compared to the electrical forces. Pease and Russel [12] have recently considered the interface between a leaky dielectric liquid and air, in order to examine the effect of nonzero conductivity in the polymer on the wavelengths and growth rates, under conditions in which gravity is unimportant. They used a long-wave analysis to derive the

linear stability equations and showed in general that the presence of conductivity in the polymer film decreases the length scale significantly, and increases the growth rate by several orders of magnitude.

However, previous studies have not addressed the following issues that could have important implications in pattern formation applications: What is the effect of the viscosity ratio between the two fluids on $\lambda_{\max}$ for the interface between a perfect and a leaky dielectric fluid? The configuration where both the fluids are viscous, and have nonzero conductivities, has not been analyzed thus far. In this case, does the viscosity ratio have any effect on $\lambda_{\max}$? To what extent is the length scale reduced when both the fluids are leaky dielectrics? How does $\lambda_{\max}$ vary with the ratio of the thickness of the two fluid layers? In order to answer these questions, we undertake a linear stability analysis of the most general case, viz. two leaky dielectric fluids of arbitrary conductivities and viscosities, and examine the effect of various system parameters on $\lambda_{\max}$ and the growth rate of the most unstable modes. The rest of this paper is organized in the following manner: Section 2.1 discusses the relevant governing equations, boundary conditions, and nondimensionalization. In Section 2.2 we outline the long-wave asymptotic analysis used to derive the nonlinear evolution equations for the interface position and charge, and in Section 2.3 we develop the linear stability analysis of the nonlinear equations. Section 3 summarizes the important representative results obtained from the linear stability analysis for both perfect dielectric–leaky dielectric and leaky dielectric–leaky dielectric interfaces. Finally, the salient conclusions of the present study are discussed in Section 4.

2. Problem formulation

The system of interest consists of two leaky dielectric fluids of arbitrary viscosities occupying the region $-H < y < 0$ (fluid 2) and $0 < y < \beta H$ (fluid 1) in the initial unperturbed state (see Fig. 1), where β is the ratio of the thicknesses of top and bottom fluids. The perturbed interface between the two fluids is denoted by $y = h(x)$. The two fluids are stationary in the initial state, with viscosities μ_i, dielectric constants ϵ_i, and conductivities σ_i, where $i = 1, 2$. Fluid 2 is bounded at the bottom $y = -H$ by a rigid plate which is maintained at a potential $\psi = \psi_b$, while fluid 1 is bounded at the top by $y = \beta H$ by a rigid plate maintained at a potential $\psi = 0$. In the ensuing analysis, we assume that the material properties of the fluid such as viscosities μ_i, dielectric constants ϵ_i and conductivities σ_i are constant, and independent of spatial position. Following the leaky dielectric model formulation of Saville [3], we assume that electroneutrality is valid in the bulk, while free charge is assumed to accumulate at the fluid interface. We also neglect the diffusion of free charge within the interface. The rest of this section is organized into three subsections which respectively deal with (1) the presentation of governing equations, boundary conditions, and nondimensionalization, (2) derivation of the nonlinear evolution equation for the interface position and interfacial free charge using a long-wave asymptotic analysis, and (3) the linear stability analysis of this coupled set of nonlinear evolution equations. We closely follow Saville's [3] review on this subject for the development of governing equations and boundary conditions.

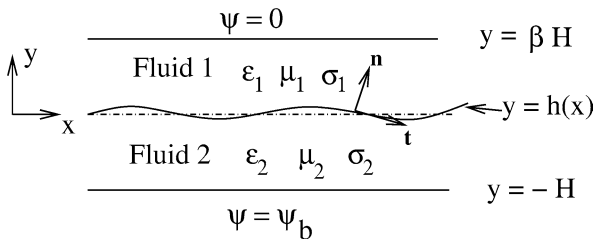

Fig. 1. Schematic diagram showing the configuration and coordinate system considered in Section 2.

2.1. Governing equations

For leaky dielectric fluids of constant conductivities and with zero net charge in the bulk, the following governing equations are appropriate for the electric field **E** in the two fluids 1 and 2 [3]:

$$\nabla \cdot \mathbf{E}_i = 0, \quad i = 1, 2. \tag{1}$$

Since the electric fields are irrotational, $\mathbf{E}_i = -\nabla\psi_i$, where ψ_i is the potential in the fluid i. Substituting this in Eq. (1) gives the following Laplace equation for the potential ψ_i:

$$\nabla^2\psi_i = 0. \tag{2}$$

These governing equations are supplemented by the following boundary conditions. First, at the interface $y = h(x)$, the normal component of the electric field satisfies

$$\epsilon_1\epsilon_0(-\nabla\psi_1 \cdot \mathbf{n}) - \epsilon_2\epsilon_0(-\nabla\psi_2 \cdot \mathbf{n}) = q(x, t), \tag{3}$$

where **n** is the unit normal to the interface at $y = h(x)$ (see Fig. 1), ϵ_i $(i = 1, 2)$ is the dielectric constant in fluid i, ϵ_0 is the permittivity of free space, and $q(x, t)$ is the surface charge density of the free charge at the interface. The continuity of the tangential component of the electric field at the interface $y = h(x)$ translates to the continuity of the potentials

$$\psi_1 = \psi_2. \tag{4}$$

The potential satisfies the boundary conditions $\psi_2 = \psi_b$ at $y = -H$, and $\psi_1 = 0$ at $y = \beta H$.

We next turn to the equations governing the motion of the two fluids. Owing to the relatively small thicknesses of the fluids, we ignore inertial effects in both fluids, and hence the governing equations are the Stokes equations for continuity and momentum balance,

$$\nabla \cdot \mathbf{v}_i = 0, \qquad \nabla \cdot \mathbf{T}_i = 0, \tag{5}$$

where $\mathbf{v}_i$ is the velocity field in fluid i, and $\mathbf{T}_i$ is the *total* stress tensor in fluid i. We have neglected the effects of gravity on the length scales of interest here. In addition, the effects of van der Waals dispersion forces are negligible for the films considered in the experimental studies [6], which were of thickness $O(100\text{ nm})$ and higher. The total stress tensor $\mathbf{T}$ is given by a sum of isotropic pressure, deviatoric viscous stresses for the Newtonian fluid, and the electrical Maxwell stress tensor,

$$\mathbf{T}_i = -p_i\mathbf{I} + \mu_i\big(\nabla\mathbf{v}_i + \nabla\mathbf{v}_i^T\big) + \mathbf{m}_i, \quad i = 1, 2, \tag{6}$$

where p_i is the pressure in fluid i, $\mathbf{I}$ is the identity tensor, and the Maxwell stress tensor $\mathbf{m}_i$ is given by [3]:

$$\mathbf{m}_i = \epsilon_i\epsilon_0\left[\mathbf{E}_i\mathbf{E}_i - \frac{1}{2}(\mathbf{E}_i\cdot\mathbf{E}_i)\mathbf{I}\right]. \tag{7}$$

The divergence of the Maxwell stress tensor $\nabla\cdot\mathbf{m}_i = 0$ because the bulk of the fluid is free of net charge, and the dielectric constants are independent of spatial position in the two fluids. Thus, the Maxwell stress tensor will not appear in the momentum balance, but will affect the flow only through the conditions at the interface. The governing momentum equations in the two fluids therefore become

$$-\nabla p_i + \mu_i\nabla^2\mathbf{v}_i = 0, \quad i = 1, 2. \tag{8}$$

The fluid velocities satisfy no-slip and no-penetration conditions at the top and bottom plates:

$$\mathbf{v}_1(y = \beta H) = 0, \qquad \mathbf{v}_2(y = -H) = 0. \tag{9}$$

At the interface $y = h(x)$ between the two fluids, continuity of velocities and stresses apply,

$$(\mathbf{v}\cdot\mathbf{n})_1 = (\mathbf{v}\cdot\mathbf{n})_2, \tag{10}$$

$$(\mathbf{v}\cdot\mathbf{t})_1 = (\mathbf{v}\cdot\mathbf{t})_2, \tag{11}$$

$$(\mathbf{n}\cdot\mathbf{T}\cdot\mathbf{n})_2 = (\mathbf{n}\cdot\mathbf{T}\cdot\mathbf{n})_1 + \gamma\kappa, \tag{12}$$

$$(\mathbf{t}\cdot\mathbf{T}\cdot\mathbf{n})_2 = (\mathbf{t}\cdot\mathbf{T}\cdot\mathbf{n})_1, \tag{13}$$

where γ is the interfacial tension between the two fluids, $\mathbf{t}$ is the unit tangent to the interface (see Fig. 1), and κ is the mean curvature of the interface. We restrict our attention to two-dimensional systems which are invariant in the z direction and denote the velocity components in the x and y direction by u and v, respectively: $\mathbf{v}_i = (u_i, v_i)$. Upon substituting the expression for the Maxwell stress tensor (7) in (12) and (13), respectively, we obtain the following conditions to be applied at the interface $y = h(x)$,

$$\begin{aligned}&\left[-p_2 + 2\mu_2\frac{\partial v_2}{\partial y}\right] - \left[-p_1 + 2\mu_1\frac{\partial v_1}{\partial y}\right]\\ &\quad= \gamma\kappa + \frac{1}{2}\epsilon_1\epsilon_0\big[(\nabla\psi_1\cdot\mathbf{n})^2 - (\nabla\psi_2\cdot\mathbf{t})^2\big]\\ &\qquad- \frac{1}{2}\epsilon_2\epsilon_0\big[(\nabla\psi_2\cdot\mathbf{n})^2 - (\nabla\psi_2\cdot\mathbf{t})^2\big],\end{aligned} \tag{14}$$

for the normal stress continuity, and

$$\begin{aligned}&\mu_2\left[\frac{\partial u_2}{\partial y} + \frac{\partial v_2}{\partial x}\right] - \mu_1\left[\frac{\partial u_1}{\partial y} + \frac{\partial v_1}{\partial x}\right]\\ &\quad= (-\nabla\psi_1\cdot\mathbf{t})q(x, t),\end{aligned} \tag{15}$$

for the tangential stress continuity. In the last equation, we have used the normal electric field continuity condition, Eq. (3), to simplify the right-hand side. The kinematic condition at the interface prescribes the evolution of the interface position $h(x, t)$,

$$v_1\big(y = h(x)\big) = v_2\big(y = h(x)\big) = \frac{\partial h}{\partial t} + \mathbf{v}\cdot\nabla_s h, \tag{16}$$

where ∇_s is the gradient operator along the interface $y = h(x)$. Finally, the interfacial charge is governed by a conservation equation,

$$\begin{aligned}&\frac{\partial q}{\partial t} + \mathbf{v}\cdot\nabla_s q - q\mathbf{n}\cdot(\mathbf{n}\cdot\nabla)\mathbf{v}\\ &\quad= [-\sigma_1\mathbf{E}_1\cdot\mathbf{n}] - [-\sigma_2\mathbf{E}_2\cdot\mathbf{n}],\end{aligned} \tag{17}$$

where the terms on the left side represent respectively the accumulation, convection, and variation of the charge due to dilation of the interface, while the right side represents the migration of charge to or from the interface due to ion conduction in the bulk [3].

It is useful at this point to nondimensionalize the governing equations and boundary conditions. The following scales are used for this purpose: ψ_b for potentials, $\epsilon_0\psi_b^2/H^2$ for pressure and stresses, H for lengths, $1/H$ for derivatives, ψ_b/H for electric fields, $\epsilon_0\psi_b^2/(\mu_2 H)$ for velocities, $\mu_2 H^2/(\epsilon_0\psi_b^2)$ for time, $\epsilon_0\psi_b/H$ for interfacial charge, and $\epsilon_0\psi_b^2/H$ for the interfacial tension. Upon using these scales to nondimensionalize the above governing equations and boundary conditions, we end up with the following nondimensional set of equations. Without loss of clarity, and for the sake of brevity, *we represent nondimensional variables with the same notation in the ensuing discussion, without any subscripts or superscripts*. The rest of this paper will deal only with nondimensional variables, unless stated otherwise explicitly.

The nondimensional governing equations for the potential ψ_i are

$$\nabla^2\psi_i = 0, \quad i = 1, 2, \tag{18}$$

with the following conditions at the interface $y = h(x)$,

$$[-\epsilon_1\nabla\psi_1\cdot\mathbf{n}] - [-\epsilon_2\nabla\psi_2\cdot\mathbf{n}] = q, \qquad \psi_1 = \psi_2, \tag{19}$$

and the following boundary conditions at the top and bottom boundaries:

$$\psi_1(y = \beta) = 0, \qquad \psi_2(y = -1) = 1. \tag{20}$$

Similarly, the nondimensional equations governing the fluid motion are

$$\begin{aligned}&\nabla\cdot\mathbf{v}_1 = 0, \qquad \nabla\cdot\mathbf{v}_2 = 0,\\ &-\nabla p_1 + \mu_r\nabla^2\mathbf{v}_1 = 0, \qquad -\nabla p_2 + \nabla^2\mathbf{v}_2 = 0,\end{aligned} \tag{21}$$

with $\mu - r = \mu_1/\mu_2$ being the ratio of viscosities of the two fluids. The nondimensional normal and tangential stress continuity conditions at the interface become

$$\left[-p_2 + 2\frac{\partial v_2}{\partial y}\right] - \left[-p_1 + 2\mu_r \frac{\partial v_1}{\partial y}\right] = \overline{\gamma}\kappa + \frac{1}{2}\epsilon_1\left[(\nabla\psi_1 \cdot \mathbf{n})^2 - (\nabla\psi_2 \cdot \mathbf{t})^2\right] - \frac{1}{2}\epsilon_2\left[(\nabla\psi_2 \cdot \mathbf{n})^2 - (\nabla\psi_2 \cdot \mathbf{t})^2\right], \tag{22}$$

and

$$\left[\frac{\partial u_2}{\partial y} + \frac{\partial v_2}{\partial x}\right] - \mu_r\left[\frac{\partial u_1}{\partial y} + \frac{\partial v_1}{\partial x}\right] = (-\nabla\psi_1 \cdot \mathbf{t})q(x,t), \tag{23}$$

where $\overline{\gamma} = \gamma H/(\epsilon_0\psi_b^2)$ is the nondimensional interfacial tension. The boundary conditions for the velocities at the top and bottom plates become

$$u_1(y=\beta) = 0, \qquad v_1(y=\beta) = 0,$$
$$u_2(y=-1) = 0, \qquad v_2(y=-1) = 0. \tag{24}$$

The nondimensional kinematic condition at the interface is

$$v_1\big(y=h(x)\big) = v_2\big(y=h(x)\big) = \frac{\partial h}{\partial t} + \mathbf{v}\cdot\nabla_s h, \tag{25}$$

and the nondimensional charge conservation equation at the interface is

$$\frac{\partial q}{\partial t} + \mathbf{v}\cdot\nabla_s q - q\mathbf{n}\cdot(\mathbf{n}\cdot\nabla)\mathbf{v} = [S_1\nabla\psi_1\cdot\mathbf{n}] - [S_2\nabla\psi_2\cdot\mathbf{n}], \tag{26}$$

where $S_i = \sigma_i\mu_2 H^2/(\epsilon_0\psi_b^2)$, $i = 1, 2$, are the nondimensional conductivities in the two fluids.

This completes the specification of the governing equations and boundary conditions, which are highly coupled. Due to the negligible effect of gravity at length scales of interest here, the above system of equations undergoes a long-wave instability. We now carry out a long-wave asymptotic analysis to make the above system of equations tractable, and thereby derive coupled nonlinear evolution equations for the interface position $h(x,t)$ and charge $q(x,t)$. While the main focus of this paper is to analyze the stability of the linearized equations, it is nonetheless useful to first derive the nonlinear evolution equations, since these equations can be used in future studies to understand (by numerical simulations) the nonlinear evolution processes that occur after the linear instability.

2.2. Long-wave asymptotic analysis

In the long-wave limit, the wavelength L of the fastest growing modes is much larger than the transverse length scale H in the system, and it is useful to define a small parameter $\delta = H/L \ll 1$. The lateral length scale L is determined self-consistently in the following analysis to be $L = (\gamma H^3/\epsilon_0\psi_b^2)^{1/2}$, and this is further estimated below to be much larger than H. Similarly, a slow time scale is necessary to describe the dynamics of the interface motion at such large length scales, and this is introduced a little later in Eq. (41). In the limit $H \ll L$, the derivatives in the x direction should be scaled with L. To this end, we define the slowly varying scale $\mathcal{X}$ in the following manner,

$$\frac{\partial}{\partial x} = \delta\frac{\partial}{\partial \mathcal{X}}, \tag{27}$$

and $\partial/\partial\mathcal{X} \sim O(1)$. When we apply the above scalings, Eq. (27), to the Laplace equation, Eq. (18), for the potential ψ_i, it simplifies in the limit $\delta \ll 1$ to

$$\frac{\partial^2\psi_i}{\partial y^2} = 0, \quad i = 1, 2. \tag{28}$$

The continuity condition for the normal component of the electric field at the interface $y = h(\mathcal{X})$, Eq. (19), is similarly simplified in the long-wave limit as

$$\left[-\epsilon_1\frac{\partial\psi_1}{\partial y}\right] - \left[-\epsilon_2\frac{\partial\psi_2}{\partial y}\right] = q, \tag{29}$$

while the other interface condition (second equation in Eq. (19)) and the boundary conditions, Eq. (20), remain unchanged in the long-wave limit.

We now turn to the simplification of the momentum equations (Eq. (21)) for the fluid motion in the long-wave limit. It is useful to define the variable $\mu_{r,i}$ such that $\mu_{r,i} = \mu_r$ for $i = 1$, and $\mu_{r,i} = 1$ for $i = 2$. The x-momentum equation can be simplified in the long-wave limit as

$$-\delta\frac{\partial p_i}{\partial\mathcal{X}} + \mu_{r,i}\frac{\partial^2 u_i}{\partial y^2} = 0. \tag{30}$$

This suggests that $u_i \sim O(\delta)p_i$. In order to make this explicit, and to make ordering of various quantities simpler, we represent the pressure p_i and the x-component velocity u_i in the following manner:

$$p_i = p_i^{(0)}, \qquad u_i = \delta u_i^{(0)}. \tag{31}$$

The above variables are the leading order quantities in an asymptotic expansion in δ, and we will be concerned only with the leading order variables in this paper. The continuity equation in both fluids (21) becomes, upon using $\partial/\partial x \sim \delta\partial/\partial\mathcal{X}$, and using the above expansion for u_i,

$$\delta^2\frac{\partial u_i^{(0)}}{\partial\mathcal{X}} + \frac{\partial v_i}{\partial y} = 0, \tag{32}$$

which suggests the following expansion for v_i:

$$v_i = \delta^2 v_i^{(0)}. \tag{33}$$

Upon using this expansion, the nondimensional y component of the momentum equation yields, to leading order in δ, $\partial p_i^{(0)}/\partial y = 0$, implying that the pressure is constant in both films across the y direction, and so $p_i = p_i(\mathcal{X}, t)$. The

simplified x-momentum equation, therefore, is given by

$$\frac{-dp_i^{(0)}}{d\mathcal{X}} + \mu_{r,i}\frac{\partial^2 u_i^{(0)}}{\partial y^2} = 0. \tag{34}$$

The normal stress condition at the interface, Eq. (22), simplifies to give the following equation in the long-wave limit:

$$\left(-p_2^{(0)}\right) - \left(-p_1^{(0)}\right) = \overline{\gamma}\delta^2\frac{\partial^2 h}{\partial \mathcal{X}^2} + \frac{1}{2}\epsilon_1\left(\frac{\partial \psi_1}{\partial y}\right)^2 - \frac{1}{2}\epsilon_2\left(\frac{\partial \psi_2}{\partial y}\right)^2. \tag{35}$$

In order for the interfacial tension to be of the same order as the other terms in the above equation, we require $\overline{\gamma}\delta^2 \sim O(1)$, where $\delta = H/L$. We set $\overline{\gamma}(H/L)^2 = 1$, and from this relation, we determine the lateral length scale L to be $L = (\overline{\gamma}H^2)^{1/2} = (\gamma H^3/\epsilon_0\psi_b^2)^{1/2}$. Upon using the relation $\overline{\gamma}\delta^2 = 1$, Eq. (35) becomes

$$\left(-p_2^{(0)}\right) - \left(-p_1^{(0)}\right) = \frac{\partial^2 h}{\partial \mathcal{X}^2} + \frac{1}{2}\epsilon_1\left(\frac{\partial \psi_1}{\partial y}\right)^2 - \frac{1}{2}\epsilon_2\left(\frac{\partial \psi_2}{\partial y}\right)^2. \tag{36}$$

The tangential stress continuity, Eq. (23), simplifies to the following condition in the long-wave limit:

$$\frac{\partial u_2^{(0)}}{\partial y} - \mu_r\frac{\partial u_1^{(0)}}{\partial y} = -q\frac{\partial \psi_1}{\partial \mathcal{X}}. \tag{37}$$

The nondimensional kinematic condition at the interface, Eq. (25) yields, after using the asymptotic expansion for v_i (Eq. (33)):

$$\delta^2 v_1^{(0)}\big(y = h(x)\big) = \frac{\partial h}{\partial t} + \delta^2 u_1^{(0)}\frac{\partial h}{\partial \mathcal{X}}. \tag{38}$$

In order for the time derivative term in the above equation to be of the same order as the other two terms, it is necessary to stipulate a slow time scale in the long-wave limit, such that

$$\frac{\partial}{\partial t} = \delta^2\frac{\partial}{\partial \tau}, \tag{39}$$

where $\partial/\partial\tau$ is $O(1)$. The kinematic condition thus gives

$$v_1^{(0)}\big(y = h(\mathcal{X})\big) = \frac{\partial h}{\partial \tau} + u_1^{(0)}\frac{\partial h}{\partial \mathcal{X}}. \tag{40}$$

The dimensional slow time scale is obtained as follows,

$$\frac{\partial}{\partial t} = \frac{\mu_2 H^2}{\epsilon_0\psi_b^2}\frac{\partial}{\partial t_{\mathrm{dim}}} = \delta^2\frac{\partial}{\partial \tau}, \tag{41}$$

where t_{dim} is the dimensional time. Thus, in order to nondimensionalize the dimensional time t_{dim} in the long-wave limit, the appropriate time scale is $\mu_2 H^2/(\epsilon_0\psi_b^2\delta^2)$. After using $\overline{\gamma}\delta^2 = 1$ to eliminate δ^2, the time scale becomes $\mu_2 H^3\gamma/(\epsilon_0\psi_b^2)^2$.

Finally, the nondimensional interfacial charge balance, Eq. (26) is simplified in the long-wave limit as

$$\delta^2\frac{\partial q}{\partial \tau} + \delta^2 u_1^{(0)}\frac{\partial q}{\partial \mathcal{X}} - q\delta^2\frac{\partial v_1^{(0)}}{\partial y} = S_1\frac{\partial \psi_1}{\partial y} - S_2\frac{\partial \psi_2}{\partial y}. \tag{42}$$

The above equation suggests that the nondimensional conductivities S_1 and S_2 both should scale as δ^2 in order to balance the left side of the equation. So, we let $S_i = S_i^{(0)}\delta^2$, $i = 1, 2$, where $S_i^{(0)} = \sigma_i\mu_2\gamma H^3/(\epsilon_0^3\psi_b^4)$. Upon using these rescaled conductivities, the charge conservation equation becomes, after using the continuity equation, Eq. (32),

$$\frac{\partial q}{\partial \tau} + \frac{\partial (u_1^{(0)}q)}{\partial \mathcal{X}} = S_1^{(0)}\frac{\partial \psi_1}{\partial y} - S_2^{(0)}\frac{\partial \psi_2}{\partial y}. \tag{43}$$

This completes the derivation of the simplified governing equations in the long-wave limit.

We now outline the derivation of the nonlinear evolution equations for the interfacial position $h(\mathcal{X}, \tau)$, and surface charge density $q(\mathcal{X}, \tau)$. The simplified Laplacian for the potential ψ_i, Eq. (28), is easily solved along with the boundary conditions, Eqs. (29), to give the following expressions for the potentials ψ_i $(i = 1, 2)$,

$$\psi_1(\mathcal{X}, y) = \frac{(\beta - y)(\epsilon_2 + (1 + h(\mathcal{X}))q(\mathcal{X}))}{\epsilon_1 + \beta\epsilon_2 + (\epsilon_1 - \epsilon_2)h(\mathcal{X})}, \tag{44}$$

and

$$\psi_2(\mathcal{X}, y) = \big[\beta\epsilon_2 - \epsilon_1 y + \beta(1 + y)q(\mathcal{X}) + h(\mathcal{X})\big(\epsilon_1 - \epsilon_2 - (1 + y)q(\mathcal{X})\big)\big] \big/ \big[\epsilon_1 + \beta\epsilon_2 + (\epsilon_1 - \epsilon_2)h(\mathcal{X})\big], \tag{45}$$

where the interfacial charge density $q(\mathcal{X}, \tau)$ is determined below by the interface charge conservation equation (43). The simplified x-momentum equation (34) can be integrated with respect to y since $dp_i^{(0)}/d\mathcal{X}$ is independent of y, and the two constants of integration that arise are determined by the boundary conditions that $u_1^{(0)}(\beta) = 0$ and $u_1^{(0)}[y = h(\mathcal{X})] = u_{\mathrm{int}}^{(0)}(\mathcal{X})$, and similarly for fluid 2, $u_2^{(0)}(-1) = 0$ and $u_2^{(0)}[y = h(\mathcal{X})] = u_{\mathrm{int}}^{(0)}(\mathcal{X})$. Here, $u_{\mathrm{int}}(\mathcal{X})$ is the x component of the velocity at the interface $y = h(\mathcal{X})$, and this quantity will eventually be determined by using the tangential stress continuity condition, Eq. (37). For the purposes of keeping the algebra tractable, it is found convenient to keep $u_{\mathrm{int}}^{(0)}(\mathcal{X})$ undetermined at present.

The solutions for the x-component velocities $u_i^{(0)}$ $(i = 1, 2)$ thus obtained are

$$u_1^{(0)}(\mathcal{X}, y) = (\beta - y)\Big[2\mu_r u_{\mathrm{int}}^{(0)}(x) + \big(\beta - h(\mathcal{X})\big)\big(-y + h(\mathcal{X})\big)\frac{dp_1^{(0)}(\mathcal{X})}{d\mathcal{X}}\Big] \Big/ \big[2\mu_r\big(\beta - h(\mathcal{X})\big)\big], \tag{46}$$

and

$$u_2^{(0)}(\mathcal{X},y)=(1+y)\Bigg[2u_{\rm int}^{(0)}(x)+\big(y-h(\mathcal{X})\big)\big(1+h(\mathcal{X})\big)\frac{dp_2^{(0)}(\mathcal{X})}{d\mathcal{X}}\Bigg]\Big/\big[2\big(1+h(\mathcal{X})\big)\big], \tag{47}$$

where the pressure gradients $dp_i^{(0)}/d\mathcal{X}$ $(i=1,2)$ are determined below.

The continuity equation (32), after substituting the asymptotic expansion for v_i, Eq. (33), simplifies to

$$\frac{\partial u_i^{(0)}}{\partial\mathcal{X}}+\frac{\partial v_i^{(0)}}{\partial y}=0. \tag{48}$$

The above equation is integrated with respect to y from $y=\beta$ to $y=h(\mathcal{X})$ for fluid 1, and $y=-1$ to $y=h(\mathcal{X})$ for fluid 2, to yield the following expressions for the normal velocities at the interface $v_i^{(0)}[y=h(\mathcal{X})]$ for $i=1,2$, where the integration constant is set to zero in order to satisfy the no-penetration condition at $y=\beta$ and $y=-1$:

$$v_1^{(0)}\big[y=h(\mathcal{X})\big]=-\int_\beta^{h(\mathcal{X})}dy\,\frac{\partial u_1^{(0)}}{\partial\mathcal{X}},$$

$$v_2^{(0)}\big[y=h(\mathcal{X})\big]=-\int_{-1}^{h(\mathcal{X})}dy\,\frac{\partial u_2^{(0)}}{\partial\mathcal{X}}. \tag{49}$$

Note that the normal velocities of the two fluids are equal at the interface (normal velocity continuity condition), and so $v_1^{(0)}[y=h(\mathcal{X})]=v_2^{(0)}[y=h(\mathcal{X})]=v_{\rm int}^{(0)}$. Therefore, we equate the two integrals in the above equation and apply Leibnitz rule:

$$\frac{\partial}{\partial\mathcal{X}}\int_\beta^{h(\mathcal{X})}u_1^{(0)}\,dy-\frac{\partial h}{\partial\mathcal{X}}u_1^{(0)}\big[h(\mathcal{X})\big]=\frac{\partial}{\partial\mathcal{X}}\int_{-1}^{h(\mathcal{X})}u_2^{(0)}\,dy-\frac{\partial h}{\partial\mathcal{X}}u_2^{(0)}\big[h(\mathcal{X})\big]. \tag{50}$$

Noting that the x-component velocities are equal at the interface, $u_1^{(0)}[h(\mathcal{X})]=u_2^{(0)}[h(\mathcal{X})]$, the above equation is simplified to

$$\frac{\partial}{\partial\mathcal{X}}\left[\int_\beta^{h(\mathcal{X})}u_1^{(0)}\,dy-\int_{-1}^{h(\mathcal{X})}u_2^{(0)}\,dy\right]=0. \tag{51}$$

We next integrate the above equation with $\mathcal{X}$, and set the integration constant (which is at most a function of time) to zero. The constant of integration is zero because the pressure gradients $dp_i^{(0)}/d\mathcal{X}$ in the two fluids should be zero in the absence of electric field, and when the interfaces are flat. We then substitute the expressions for $u_i^{(0)}(y)$ (Eqs. (46) and (47)) in the above equation, carry out the integrations with y, and substitute the simplified normal stress continuity condition (36) to eliminate $dp_2^{(0)}/d\mathcal{X}$ in terms of $dp_1^{(0)}/d\mathcal{X}$. Prior to determining $dp_1^{(0)}/d\mathcal{X}$, it is useful to determine the x component of the fluid velocity at the interface $u_{\rm int}^{(0)}$ from the simplified tangential stress continuity condition, Eq. (37). Once $u_{\rm int}^{(0)}$ is determined, the pressure gradient $dp_1^{(0)}/d\mathcal{X}$ is determined from the integrated version of Eq. (51), and thus the velocity profile (Eqs. (46) and (47)), is known completely. The expressions for $u_{\rm int}^{(0)}$ and $dp_1^{(0)}/d\mathcal{X}$ are very lengthy and are not reproduced here. We used the symbolic computation package Mathematica to perform our calculations.

Finally, the kinematic condition at the interface, Eq. (40), is used to derive the evolution equation for $h(\mathcal{X},\tau)$, as follows. We first substitute the expression for the normal fluid velocity at the interface, Eq. (49), after using Leibnitz rule on the integral,

$$\frac{\partial h}{\partial\tau}+u_1^{(0)}\big[h(\mathcal{X})\big]\frac{\partial h}{\partial\mathcal{X}}=-\frac{\partial}{\partial\mathcal{X}}\int_\beta^{h(\mathcal{X})}u_1^{(0)}\,dy+u_1^{(0)}\big[h(\mathcal{X})\big]\frac{\partial h}{\partial\mathcal{X}}, \tag{52}$$

which is simplified to give the equation

$$\frac{\partial h}{\partial\tau}+\frac{\partial}{\partial\mathcal{X}}\int_\beta^{h(\mathcal{X})}u_1^{(0)}\,dy=0, \tag{53}$$

where $u_1^{(0)}$ is substituted from Eq. (46), after using the expressions for $dp_1^{(0)}/d\mathcal{X}$ and $u_{\rm int}^{(0)}$ determined using the procedure outlined above. The evolution equation for the interfacial charge density $q(\mathcal{X},\tau)$ is obtained from Eq. (43) after substituting the expressions for $u_{\rm int}^{(0)}$ and the gradients of the potential (from Eqs. (44) and (45)) in that equation. The nonlinear evolution equations for $h(\mathcal{X},\tau)$ and $q(\mathcal{X},\tau)$ are very lengthy, and so we do not provide them here. However, in Appendix A, we provide the complete nonlinear evolution equations for $h(\mathcal{X},\tau)$ and $q(\mathcal{X},\tau)$ when the values of the parameters ϵ_1, ϵ_2, μ_r, and β are specified.

These coupled nonlinear equations can be solved numerically with appropriate initial conditions to determine the evolution of the interface in the presence of electric fields. In the present work, however, we restrict ourselves to studying the linear stability properties of these equations, an issue we turn to next.

2.3. Linear stability analysis

Before linearizing the coupled nonlinear equations, it is necessary to first determine the base state about which we perturb. The steady base state we consider is that of stationary fluids with a flat interface $h(\mathcal{X},\tau)=0$, and with a constant interfacial charge density q_0 which is independent

of $\mathcal{X}$ and τ. This base state interfacial charge q_0 is determined from Eq. (43) with the left side set to zero, since $\partial/\partial\tau = 0$ and $u_i^{(0)} = 0$ in the base state:

$$S_1^{(0)}\left[\frac{\partial\psi_1}{\partial y}\right]_{y=0} = S_2^{(0)}\left[\frac{\partial\psi_2}{\partial y}\right]_{y=0}. \tag{54}$$

The derivatives of the potentials in the above equation are calculated from Eqs. (44) and (45), with $h(\mathcal{X})$ set to zero. This yields the following expression for the steady interfacial charge density:

$$q_0 = \frac{S_2^{(0)}\epsilon_1 - \epsilon_2 S_1^{(0)}}{S_1^{(0)} + \beta S_2^{(0)}}. \tag{55}$$

The variables h and q are now perturbed about their base state values: $h(\mathcal{X},\tau) = h'\exp[ik\mathcal{X} + s\tau]$ and $q(\mathcal{X},\tau) = q_0 + q'\exp[ik\mathcal{X} + s\tau]$, where h' and q' are the amplitudes of the perturbations (which are independent of $\mathcal{X}$ and τ), k is the nondimensional wavenumber based on the lateral length scale $L = (\gamma H^3/\epsilon_0\psi_b^2)^{1/2}$ and s is the nondimensional growth rate based on the time scale $\mu_2 H^3\gamma/(\epsilon_0\psi_b^2)^2$. The coupled nonlinear evolution equations are linearized with respect to h' and q' and this results in a set of linear homogeneous equations for h' and q'. This is written in the matrix form $\mathbf{M}\cdot\mathbf{C}^T = 0$, where the vector $\mathbf{C} = [h', q']$, and the determinant of this matrix $\mathbf{M}$ is set to zero for nontrivial solutions in order to obtain the characteristic equation for s. This characteristic equation, which gives the growth rate s as a function of k, β, μ_r, $S_1^{(0)}$, $S_2^{(0)}$, ϵ_1, and ϵ_2, is a quadratic equation for s. The roots of the characteristic equation are always real, with one being always negative, and the other one can be positive or negative depending on the choice of system parameters. A typical variation of the latter root as a function of k is shown in Fig. 2. This plot confirms that the system indeed undergoes a long-wave instability, and the wavenumber of the fastest growing mode is identified as $k_{\max}$, and the growth rate of this mode is identified as $s_{\max}$. The inverse of this wavenumber $\lambda_{\max} = 2\pi/k_{\max}$ will therefore be the dominant length scale set by the linear instability. In the following section, we present results for $k_{\max}$ and $s_{\max}$ and how they vary with the system parameters ϵ_1, ϵ_2, $S_1^{(0)}$, $S_2^{(0)}$, β, and μ_r.

3. Results

We present our results in two subsections: for interfaces between perfect and leaky dielectric films, and for interfaces between two leaky dielectric films.

3.1. Perfect dielectric–leaky dielectric interface

It is first useful to recall the results for $k_{\max}$ and $s_{\max}$ for the interface between *two perfect dielectrics*, and this has been addressed in the previous studies of Russel, Steiner, and co-workers [4–7]. Their results for perfect dielectrics can be recovered from our general formulation in the previous section by setting the conductivities $S_1^{(0)} = S_2^{(0)} = 0$, and the interfacial charge $q = 0$. The wavenumber $k_{\max}$ of the fastest growing mode for the interface between two perfect dielectrics is found to be

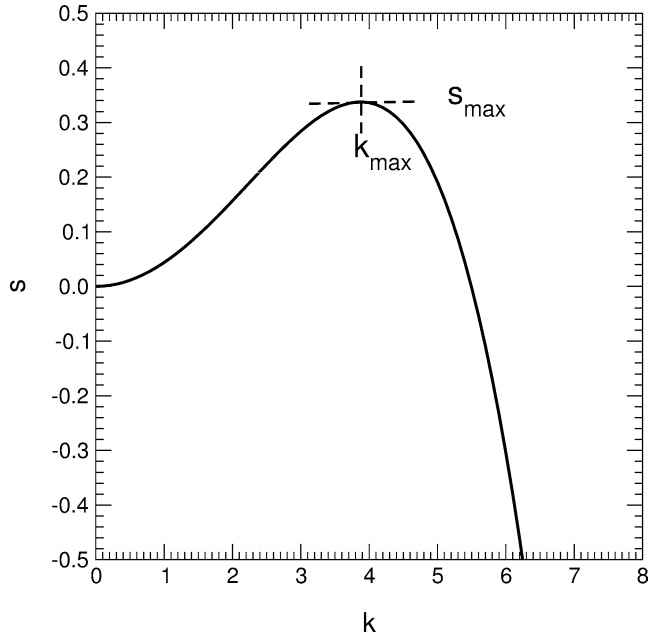

Fig. 2. A typical plot of the growth rate s as a function of wavenumber k for $S_1^{(0)} = 10^3$, $S_2^{(0)} = 10^4$, $\beta = 1/5$, $\epsilon_1 = 3$, $\epsilon_2 = 4$, $\mu_r = 1$.

$$k_{\max} = \frac{\sqrt{\epsilon_1\epsilon_2(\epsilon_1-\epsilon_2)^2}}{\sqrt{2}\sqrt{(\epsilon_1+\beta\epsilon_2)^3}}, \tag{56}$$

and the growth rate $s_{\max}$ corresponding to the fastest growing mode is given by

$$s_{\max} = \beta^3(\beta+\mu_r)\epsilon_1^2(\epsilon_1-\epsilon_2)^4\epsilon_2^2\big/\big[12\big(\beta^4 + 4\beta\mu_r + 6\beta^2\mu_r + 4\beta^3\mu_r + {\mu_r}^2\big)(\epsilon_1+\beta\epsilon_2)^6\big]. \tag{57}$$

Note that the *dimensional* expression for the wavenumber of the fastest growing mode is obtained by dividing the above expression for $k_{\max}$, Eq. (56), with the length $L = (\gamma H^3/\epsilon_0\psi_b^2)^{1/2}$, and the dimensional growth rate of the fastest growing mode is obtained by dividing $s_{\max}$ (Eq. (57)) by the time scale $\mu_2 H^3\gamma/(\epsilon_0\psi_b^2)^2$. We further recall that the instability between two perfect dielectrics vanishes when the dielectric constants are equal in the two fluids. Another interesting feature of this system is that the length scale (or, its inverse, $k_{\max}$) characteristic of the linear instability is *independent* of the viscosity of the two fluids [6]. This result can be rationalized by the observation that for perfect dielectrics, there is zero interfacial charge, and so the electric stresses drop out of the shear stress condition at the interface (see Eq. (37)). Thus, the only place where the electric stresses occur is in the normal stress condition at the interface, Eq. (36), which suggests that the instability is a competition between

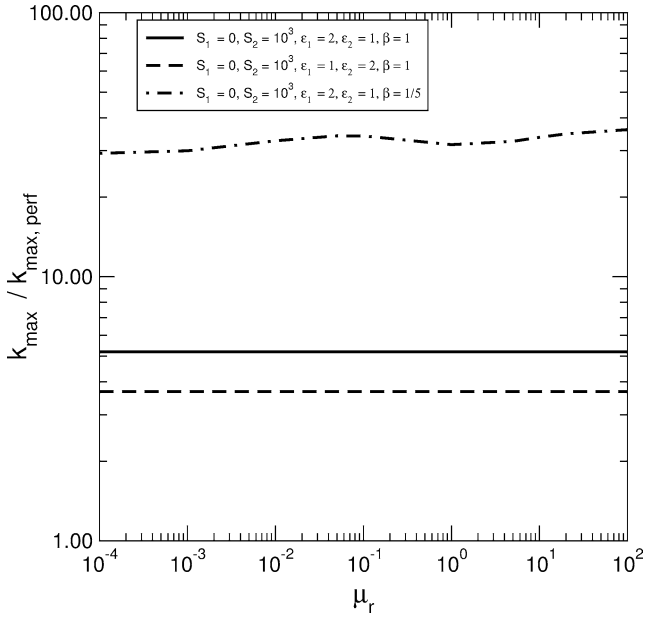

Fig. 3. Effect of the viscosity ratio μ_r on the wavenumber of the fastest growing mode for the interface between perfect and leaky dielectric films.

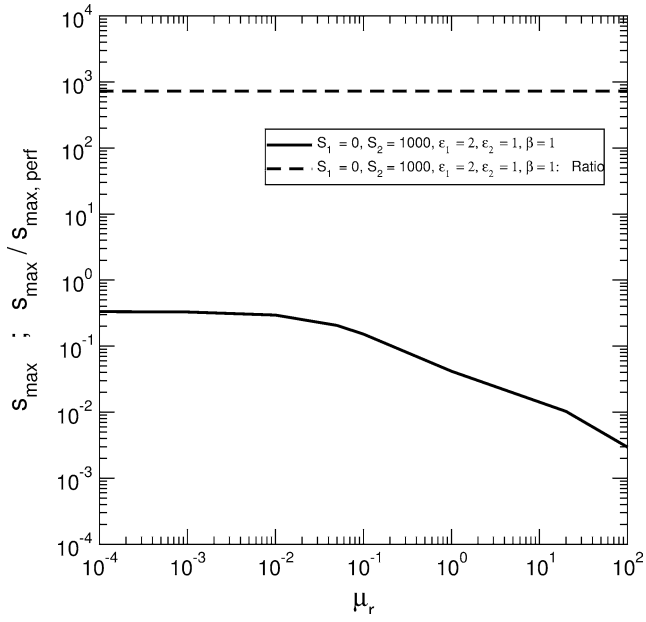

Fig. 4. Effect of the viscosity ratio μ_r on the growth rate of the fastest growing mode for the interface between perfect and leaky dielectric films: $s_{\max}$ vs μ_r and $s_{\max}/s_{\max,\text{perf}}$ vs μ_r.

the destabilizing electrical forces and stabilizing surface tension forces. Fluid viscosities do not appear in this balance, and so the length-scale characteristic of the linear instability is independent of μ_r.

We now turn to the discussion of the interface between perfect and leaky dielectric fluids of arbitrary viscosities. It is useful first to estimate the nondimensional conductivity $S_2^{(0)}$ in typical thin film applications. We choose the following set for this estimation: $H = 0.5 \times 10^{-6}$ m, $\gamma = 0.01$ N m^{-1}, $\mu_2 = 10$ N s m^{-2}, $\epsilon_0 = 8.85 \times 10^{-12}$ C^2 N^{-1} m^{-2}, $\psi_b = 1$ V, $\sigma_2 = 10^{-11}$ to 10^{-3} C^2 s kg^{-1} m^{-3}. For these set of values, $S_2^{(0)} \approx 540$ to 5×10^8, corresponding to the lower and upper limits of σ_2. Thus, the nondimensional conductivity $S_2^{(0)}$ can be made high quite easily. It is also useful to estimate the lateral length scale using the above estimates, and the ratio L/H turns out to be 25, and this is sufficiently larger than 1 to justify the long-wave analysis.

We denote perfect dielectrics by P and leaky dielectrics by L in the following discussion. A limiting case of the P–L configuration has been considered by Pease and Russel [12] who focused on the interface between a leaky dielectric liquid and air. For the system considered in [12], $\epsilon_1 = 1$, and the viscosity ratio $\mu_r \to 0$, and so the motion of the top fluid does not have any effect on the dynamics of the interface. Using the formulation given in the previous section, we first examine the effect of μ_r on $k_{\max}$ and $s_{\max}$ for the P–L interface. We denote the wavenumber of the fastest growing mode for a system of two perfect dielectrics with the same dielectric constants as that of the P–L interface by $k_{\max,\text{perf}}$. It is useful to determine the ratio of the wavenumber of the fastest growing modes for P–L and P–P interfaces, in order to examine the effect of nonzero conductivity in one of the fluids. Fig. 3 shows the variation of the ratio $k_{\max}/k_{\max,\text{perf}}$ with μ_r for a few representative parameter sets, and this shows that μ_r has no effect for thickness ratio $\beta = 1$, while its effect is only marginal for $\beta = 1/5$. However, as also noted by Pease and Russel [12], the ratio $k_{\max}/k_{\max,\text{perf}}$ can be as large as 30, meaning a $1/30$ reduction in the length-scale characteristic of the linear instability for the P–L interface, when compared to the P–P interface. The effect of μ_r on the growth rate ($s_{\max}$) of the fastest growing mode for the P–L interface, and on the ratio of the growth rates for P–L and P–P configurations, $s_{\max}/s_{\max,\text{perf}}$, is shown in Fig. 4. This shows that while $s_{\max}$ decreases with an increase in μ_r, the ratio $s_{\max}/s_{\max,\text{perf}}$ remains unchanged with an increase in μ_r. Thus, the effect of the viscosity of fluid 1 in P–L interface is identical to its effect on P–P interface. The growth rate of the fastest growing mode is typically very large (factors of $\sim 10^3$ larger, for example) for P–L interfaces when compared to that of P–P interfaces.

We next turn to the case where fluid 1 is a perfect dielectric ($S_1^{(0)} = 0$) and fluid 2 is a leaky dielectric with $S_2^{(0)} \gg 1$, but $\epsilon_1 = \epsilon_2$. When $\epsilon_1 = \epsilon_2$, there is no instability for P–P interfaces. Also, we recall that for P–P interfaces, the result for $k_{\max}$ (Eq. (56)) shows that $k_{\max} \propto (\epsilon_1 - \epsilon_2)$. However, for P–L interfaces, there is an instability even when $\epsilon_1 = \epsilon_2$, and the variation of $k_{\max}$ with μ_r for different values of ϵ_1 ($= \epsilon_2$) is shown in Fig. 5. The wavenumber of the fastest growing mode, $k_{\max}$, does not vary significantly with μ_r. This result shows that even if the contrast in dielectric constants between the two fluids is very small, a significant reduction in the length-scale characteristic of the linear instability can be achieved by making one of the fluids slightly conducting. We have also considered the variation of $k_{\max}$ with μ_r for the P–L interface, when $S_1^{(0)} = 0$, $\epsilon_1 = 1$, and for differ-

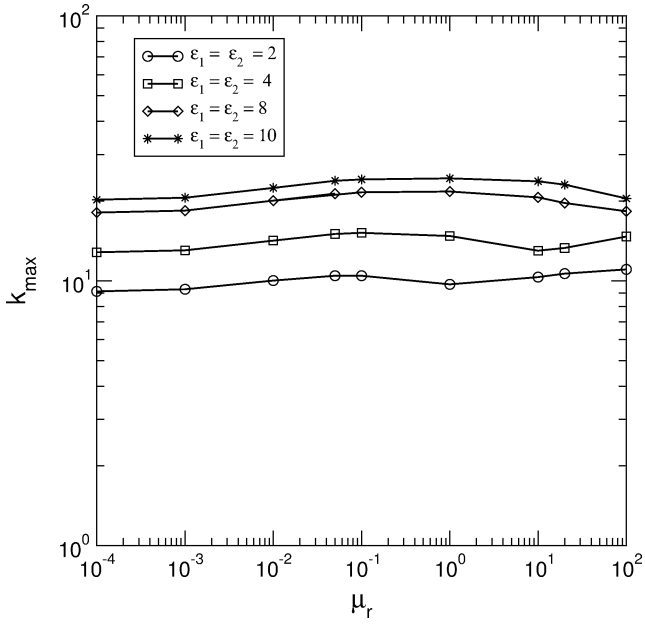

Fig. 5. Effect of the viscosity ratio μ_r on the wavenumber of the fastest growing mode for the interface between perfect and leaky dielectric films, when $\epsilon_1 = \epsilon_2$, for $S_1^{(0)} = 0$, $S_2^{(0)} = 10^3$, $\beta = 1/5$.

ent values of $S_2^{(0)}$ and ϵ_2. Our results show that varying $S_2^{(0)}$ from 1 to 10^3 has no effect on $k_{\max}$, nor does the variation of ϵ_2 and μ_r.

It is pertinent here to remark on the special case when $S_1^{(0)} = 0$, and the process of making $S_2^{(0)}$ very small, a case considered in [12]. Let us further set (without loss of generality) $\epsilon_1 = 1$, although the discussion is valid for any ϵ_1. When we set $S_1^{(0)} = 0$, and $\epsilon_1 = 1$, the interfacial charge q_0 in the base state, Eq. (55), becomes

$$q_0 = \frac{1}{\beta}, \tag{58}$$

and this is independent of $S_2^{(0)}$ and ϵ_2. Now, having this as the base state charge density at the interface, it is possible to carry out the linear stability analysis by setting $\epsilon_2 = 1$, and $S_2^{(0)} \ll 1$, or even $S_2^{(0)} = 0$ (the case of two perfect dielectrics with equal dielectric constants), and this will reveal an instability. Whereas, it is expected that for two perfect dielectrics with $\epsilon_1 = \epsilon_2$, there should be no instability. The fallacy lies in how we take the limits of the conductivities going to zero. When we let both $S_1^{(0)} = S_2^{(0)} = 0$ simultaneously at the outset, we of course obtain the case of P–P interface, as the base state charge density is zero at the interface. However, when we set $S_1^{(0)} = 0$ first, then while calculating the base state interfacial charge, Eq. (58), we implicitly assume that $S_2^{(0)} \neq 0$, and so it is possible to establish this base state charge density. Now, what happens to the case when $S_2^{(0)}$ is not zero but extremely small, $S_2^{(0)} \ll 1$? For this case, in principle, the base state charge density q_0 (Eq. (58)) can be achieved, but to reach this steady state, it is going to take a very long time, as can be verified from the interfacial charge balance, Eq. (43), with $u_{\text{int}}^{(0)} = 0$, and $S_1^{(0)} = 0$,

$$\frac{\partial q_0}{\partial \tau} = -S_2^{(0)} \frac{\partial \psi_2}{\partial y}, \tag{59}$$

which can be easily solved to estimate the time evolution of the base state charge density for a flat interface with the initial condition that at $\tau = 0$, the charge at the interface is zero:

$$q_0(\tau) = \frac{1 - \exp\left[-\left(\frac{\beta S_2^{(0)} \tau}{1+\beta}\right)\right]}{\beta}. \tag{60}$$

When we consider the limit $S_2^{(0)} \ll 1$ in the above equation, it is clear that it is going to take a large time scale $\propto 1/S_2^{(0)}$ to reach the steady-state charge density given by Eq. (58) at the interface. Therefore, for $S_1^{(0)} = 0$ and $S_2^{(0)} \ll 1$, the results of the linear stability analysis (which assumes that the steady-state charge density given by Eq. (58) is established) are suspect, given that the establishment of the steady-state charge density is a very slow process.

To illustrate this point further, we consider the interface between a leaky dielectric (with scaled conductivity $S_2^{(0)}$ and dielectric constant $\epsilon_2 \neq 1$), and air (a perfect dielectric, with $\mu_r \to 0$, and $\epsilon_1 = 1$). Let the thickness of both liquid and air be equal, i.e., $\beta = 1$. The time scale required for attaining the base state charge distribution (estimated from Eq. (60)) is proportional to $2/S_2^{(0)}$. Now, this system is unstable even if liquid 2 is a perfect dielectric, $S_2^{(0)} = 0$, with zero interfacial charge, and the (nondimensional) time scale for growth of the perturbations can be estimated (from Eq. (57)) to be proportional to $12(1+\epsilon_2)^6/(\epsilon_2^2(1-\epsilon_2)^4)$. If $\epsilon_2 = 10$, then this time scale becomes an $O(1)$ quantity. However, the time scale for reaching the base state charge distribution (Eq. (58)) is $O(1/S_2^{(0)})$, and when $S_2^{(0)} \ll 1$, this time could be much larger than the time required for growth of perturbations when the interfacial charge is absent (i.e., as if the liquid were to be a perfect dielectric). Thus, in this case, the instability that the system exhibits would be the one present in the case of two perfect dielectrics. When $S_2^{(0)}$ is not very small, it is possible that the two dynamic processes, viz. the development of a steady interfacial charge and the instability of the interface without the interfacial charge, could compete. When $S_1^{(0)} = 0$ and for not so large $S_2^{(0)}$, it is possible to prevent the instability that occurs even in perfect dielectrics by maintaining the difference between ϵ_1 and ϵ_2 to be small. This is because the time scale for growth of perturbations for two perfect dielectrics is proportional to $1/(\epsilon_2 - \epsilon_1)^4$, and when this time scale becomes larger than the time scale for the development of base charge distribution, then the instability that the system exhibits would correspond to that of a leaky dielectric–perfect dielectric interface.

We next turn to the variation of $k_{\max}$ and $s_{\max}$ with the ratio of thickness β for the P–L interface. Fig. 6 shows the

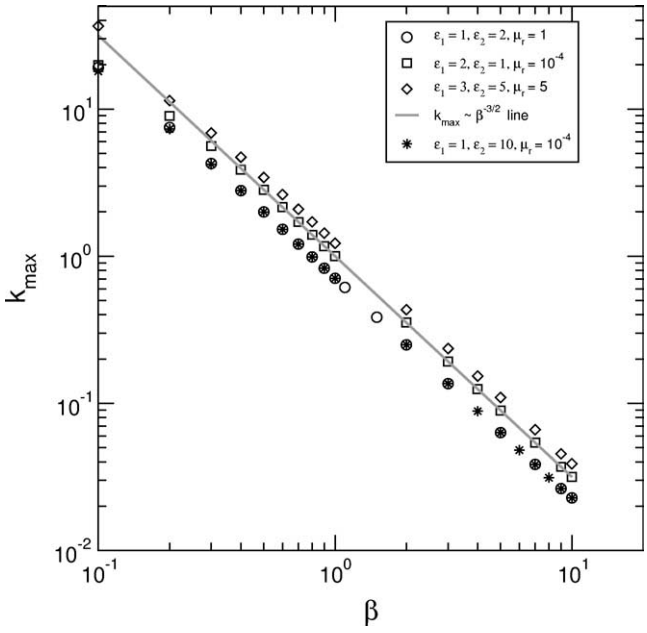

Fig. 6. Effect of the ratio of thickness β on $k_{\max}$ for the interface between perfect and leaky dielectric films: $S_1^{(0)} = 0$, $S_2^{(0)} = 10^3$.

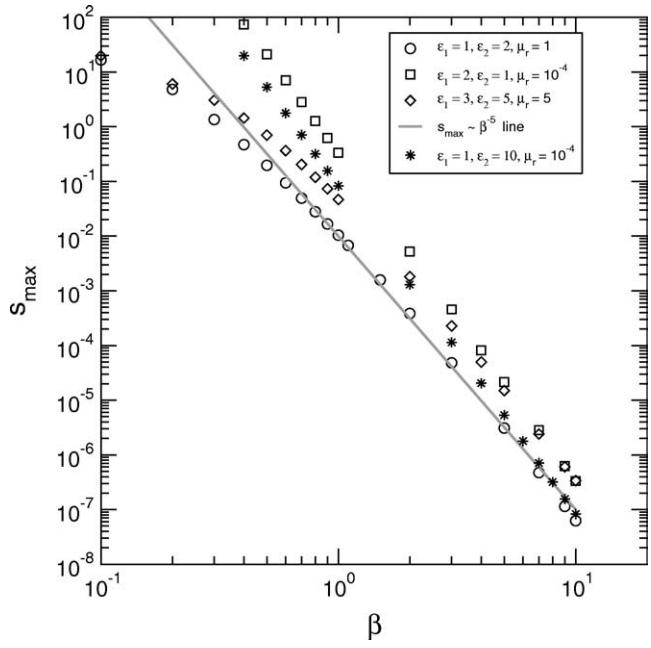

Fig. 7. Effect of the ratio of thickness β on $s_{\max}$ for the interface between perfect and leaky dielectric films: $S_1^{(0)} = 0$, $S_2^{(0)} = 10^3$.

effect of β on $k_{\max}$ for a variety of parameter sets consisting of different values of ϵ_i and μ_r, and this indicates that $k_{\max}$ decreases with β and in general $k_{\max} \propto \beta^{-3/2}$. This behavior is in agreement with the predictions of Herminghaus [11], who studied the interface between a perfect dielectric fluid of finite thickness and a leaky dielectric of much larger thickness. The results of [11] showed that $k_{\max}$ decays as $h_0^{-3/2}$, where h_0 is the thickness of the perfect dielectric layer. Similarly, Fig. 7 shows the effect of β on $s_{\max}$, and this indicates that for $\beta > 1$, the data are approximated well by $s_{\max} \propto \beta^{-5}$.

3.2. Leaky dielectric–leaky dielectric interface

We now consider the effect of various system parameters on $k_{\max}$ and $s_{\max}$ when both fluids are leaky dielectrics, i.e., L–L interface. Fig. 8 shows the typical variation of $k_{\max}$ with μ_r for two parameter sets. In marked contrast with P–P and P–L systems considered hitherto, the viscosity ratio μ_r is shown here to have a significant effect on the wavenumber of the fastest growing mode. The wavenumber decreases by a factor of 5 as μ_r is changed from 0.1 to 10. This observation is one of the main results of the present study that can be readily tested experimentally. The reason for the effect of μ_r can be discerned by noting that when both fluids are leaky dielectrics, the electrical stresses enter the tangential stress balance at the interface, which contains μ_r, which in turn influences $k_{\max}$. Fig. 9 shows that this trend prevails in L–L systems even when the dielectric constants of the two fluids are set equal. In Fig. 10, we show the effect of μ_r on $k_{\max}/k_{\max,\text{perf}}$, the ratio of the wavenumbers of the fastest growing mode for the L–L system to that of a P–P system with the same dielectric constants as the L–L system. The idea behind this comparison is to demonstrate the extent to which length scales can be reduced when there is nonzero conductivity in the two fluids, when compared to perfect dielectrics with very little contrast in their dielectric constants. Note that $k_{\max,\text{perf}}$ is independent of μ_r, and so the variation with μ_r in this figure is solely due to $k_{\max}$ for the L–L system. The inverse of this ratio is the ratio of the length scales characteristic of the linear instability, and this figure shows that the ratio of lengths can be reduced to as low as $1/50$. This prediction could have

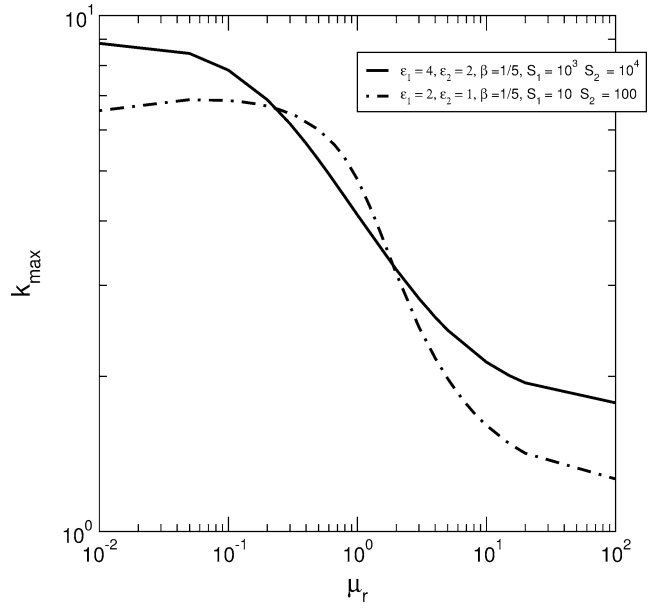

Fig. 8. Effect of viscosity ratio μ_r on $k_{\max}$ for a system consisting of two leaky dielectric fluids.

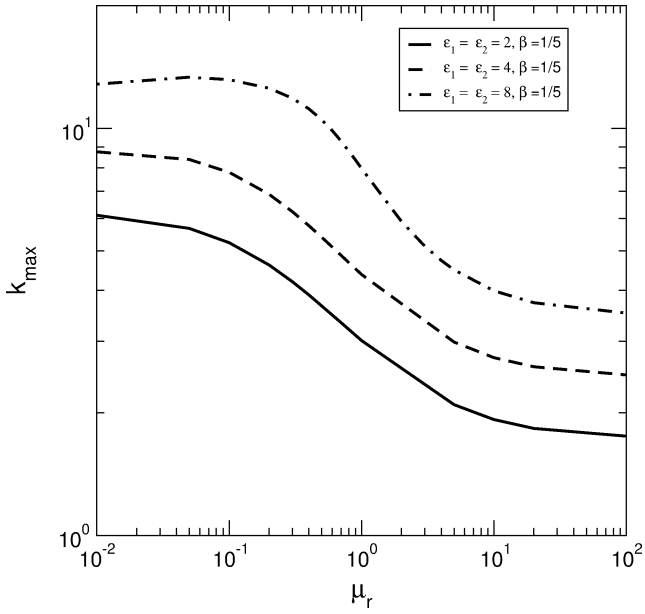

Fig. 9. Effect of viscosity ratio μ_r on $k_{\max}$ for a system consisting of two leaky dielectric fluids when $\epsilon_1 = \epsilon_2$, with $S_1^{(0)} = 10^3$ and $S_2^{(0)} = 10^4$.

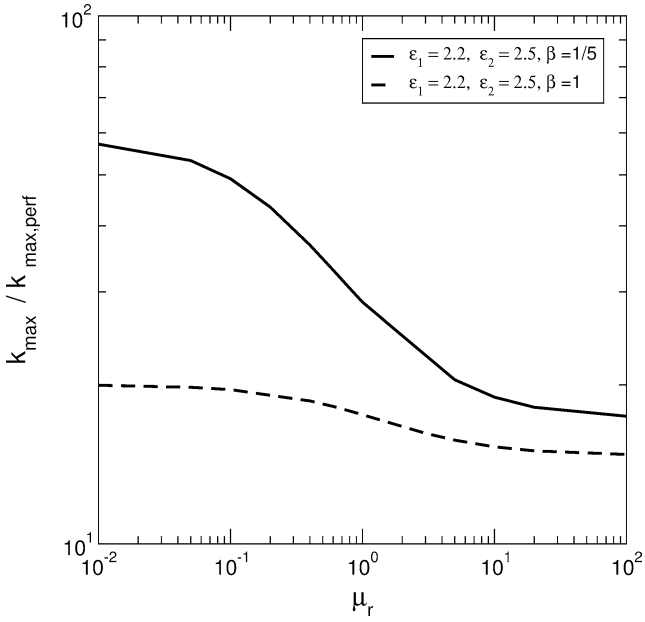

Fig. 10. Effect of viscosity ratio μ_r on $k_{\max}$ for a system consisting of two leaky dielectric fluids when $\epsilon_1 = 2.2$ and $\epsilon_2 = 2.5$, with $S_1^{(0)} = 10^3$ and $S_2^{(0)} = 10^4$.

important implications in pattern transformation using such fluids.

In Fig. 11, we show the variation of $k_{\max}$ with the thickness ratio β for different parameter sets, but all having the ratio $S_2^{(0)}/S_1^{(0)} = 10^2$. This plot indicates that $k_{\max}$ decreases with β and the variation is well approximated by $k_{\max} \propto \beta^{-3/2}$. Fig. 12 shows the same variation, but for systems with smaller conductivity ratios $S_2^{(0)}/S_1^{(0)}$, and here again the general trend is that $k_{\max}$ decreases with β, and

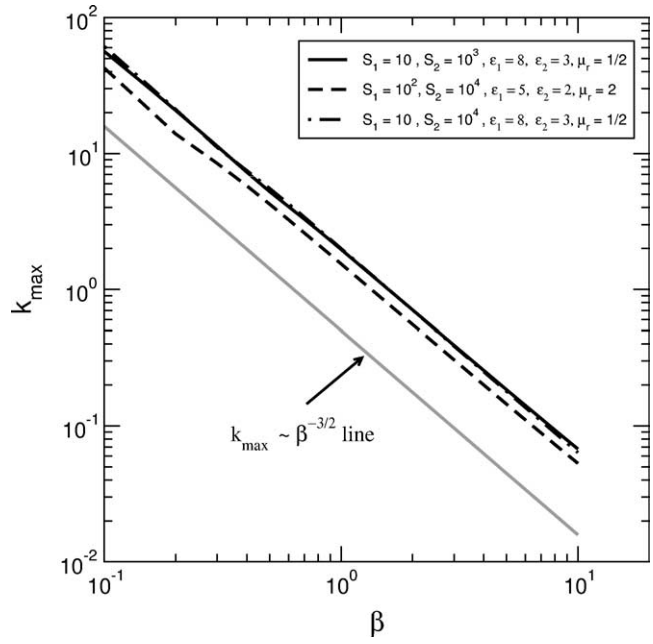

Fig. 11. Effect of thickness ratio β on $k_{\max}$ for a system consisting of two leaky dielectric fluids for various parameter sets, such that $S_2^{(0)}/S_1^{(0)} = 10^2$.

the data could be well approximated by $\beta^{-\alpha}$ where the exponent α is 5/4 for $S_2^{(0)}/S_1^{(0)} = 10$ and $\alpha = 1$ for $S_2^{(0)}/S_1^{(0)} = 2$. These two figures, along with the variation of $k_{\max}$ with β for the P–L system (Fig. 6), thus show that $k_{\max} \propto \beta^{-\alpha}$ and the exponent α is positive and increases with an increase in $S_2^{(0)}/S_1^{(0)}$ until it reaches 3/2, after which it remains constant. Figs. 13 and 14 show the variation of $s_{\max}$ with β. In general, for $\beta > 1$, $s_{\max} \propto \beta^{-\theta}$, where $\theta = 5$ for $S_2^{(0)}/S_1^{(0)} = 100$, while θ decreases to 4 when $S_2^{(0)}/S_1^{(0)} = 10$ and 15/4 for $S_2^{(0)}/S_1^{(0)} = 2$. Thus the exponent θ describing the decrease of $s_{\max}$ increases with an increase in the ratio of the conductivities $S_2^{(0)}/S_1^{(0)}$. Interestingly, as the preceding figures show, the exponents α and θ characterizing the decay of $k_{\max}$ and $s_{\max}$ depend only on the conductivity ratio $S_2^{(0)}/S_1^{(0)}$, and are largely independent of other system parameters such as ϵ_1, ϵ_2, and μ_r.

4. Conclusions

In conclusion, we have provided a general formulation for analyzing the effect of an externally applied electric field on the stability and dynamics of the interface between two leaky dielectric fluids of arbitrary viscosities and conductivities in the long-wave limit. Specific configurations studied in previous studies such as interfaces between two perfect dielectric fluids (liquid–liquid and liquid–air interfaces) and the interface between a leaky dielectric fluid and air emerge as limiting cases from the present analysis. A systematic long-wave asymptotic analysis was used to derive coupled nonlinear evolution equations for the position of the interface, and free charge density at the interface. Attention was restricted to

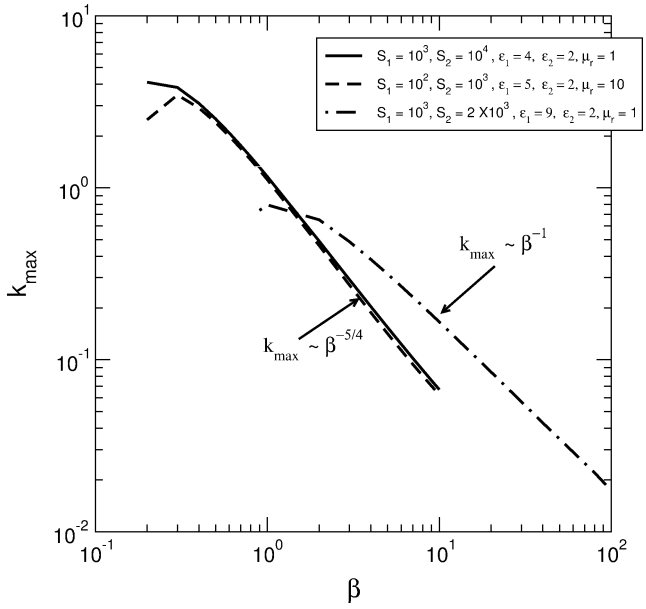

Fig. 12. Effect of thickness ratio β on $k_{\max}$ for a system consisting of two leaky dielectric fluids for various parameter sets.

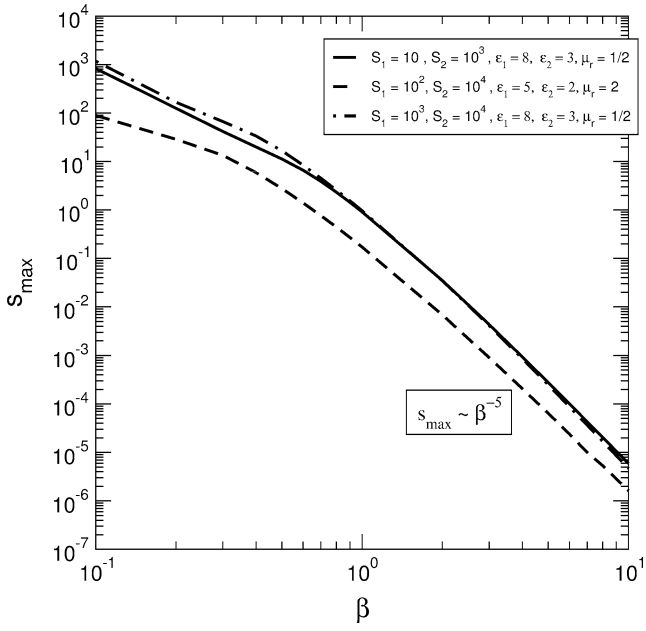

Fig. 13. Effect of thickness ratio β on $s_{\max}$ for a system consisting of two leaky dielectric fluids for various parameter sets, such that $S_2^{(0)}/S_1^{(0)} = 10^2$.

linearized stability of the coupled nonlinear equations, and the effect of a variety of system parameters on the wavelength (or, its inverse, the wavenumber $k_{\max}$) of the fastest growing mode, and the growth rate of the fastest growing mode $s_{\max}$ was studied. In general, we find that for interfaces between perfect dielectric and leaky dielectric fluids, the viscosity ratio of the two fluids does not have a significant effect on $k_{\max}$. In marked contrast, the viscosity ratio was shown to have a significant effect on $k_{\max}$ for the interface between two leaky dielectric fluids. Another important

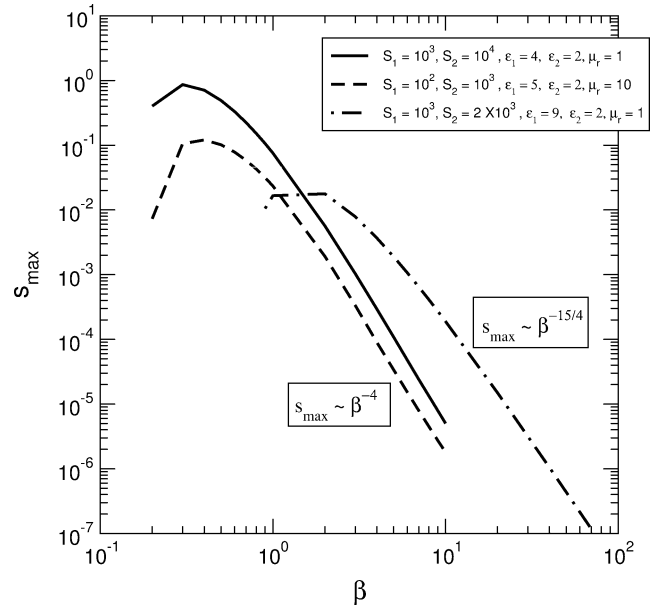

Fig. 14. Effect of thickness ratio β on $s_{\max}$ for a system consisting of two leaky dielectric fluids for various parameter sets.

feature of the interface between two leaky dielectric fluids is that the length-scale characteristic of the linear instability ($\sim 1/k_{\max}$) is significantly smaller (up to a factor of $1/50$) when compared to that of two perfect dielectric fluids. These two results, viz. the effect of viscosity ratio and the reduction of the length scale, could have important implications in pattern formation applications involving the application of electric fields to fluid interfaces.

It was further demonstrated that for the case of interfaces between perfect (fluid 1) and leaky dielectric (fluid 2) fluids, the process of taking the limit of small conductivity in the fluid 2 ($S_2^{(0)} \ll 1$) is rather subtle. In this limit, the time required to attain the base state charge distribution itself becomes large (proportional to $1/S_2^{(0)}$), and the linear stability analysis which assumes this base state charge distribution becomes suspect. Indeed, in this limit, it is possible that the system could exhibit the instability between two perfect dielectrics with zero interfacial charge, when $\epsilon_1 \neq \epsilon_2$. When $S_2^{(0)}$ is not very small, then the two dynamical processes involving the development of steady charge distribution and the growth of interfacial perturbations due to the instability between two fluids (as if they are perfect dielectrics) could compete. It is only in the case when the time for attaining the steady base state interfacial charge is rapid compared to the time scale for instability for two perfect dielectrics, that the results of Section 3.1 are rigorously valid, and the sensitivity of the instability to the conductivity of the liquid 2 is very pronounced as predicted by the theory of Pease and Russel [12].

The variation of $k_{\max}$ and $s_{\max}$ with the thickness ratio β was studied in detail, and this showed that, in general, $k_{\max}$ and $s_{\max}$ decrease with an increase in β. In particular, for $\beta > 1$, $k_{\max} \propto \beta^{-\alpha}$, and $s_{\max} \propto \beta^{-\theta}$. The exponents α and

θ depend only on the ratio of the conductivities of the two fluids, and are largely insensitive to other parameters of the system. The exponent α increases with an increase in the conductivity ratio $S_2^{(0)}/S_1^{(0)}$, reaching a saturation value of $3/2$ when the conductivity ratio reaches 100. This saturation value $3/2$ is also found to remain the same for the interface between perfect and leaky dielectric fluids, where the conductivity ratio becomes infinite. Similarly, the exponent θ characterizing the decay of $s_{\max}$ as a function of β also increases with an increase in the conductivity ratio $S_2^{(0)}/S_1^{(0)}$, reaching a saturation value of 5 when $S_2^{(0)}/S_1^{(0)}$ reaches 100. The exponent θ for the case of the interface between perfect and leaky dielectric fluids also has the same value. The nonlinear evolution of the interface under the influence of electric fields will be a subject of subsequent studies.

Appendix A. Long-wave evolution equations

In this Appendix, we provide the complete expressions for the nonlinear evolution equations ((53) and (43)). The evolution equations are derived using the symbolic package Mathematica, and they are extremely lengthy when the variables β, μ_r, ϵ_1, and ϵ_2 are unspecified. Therefore, we provide below the full nonlinear evolution equations only for the case when the values of these variables are specified. We choose, $\epsilon_1 = 2$, $\epsilon_2 = 1$, $\mu_r = 2$, $\beta = 1$ to this end.

The evolution equation for the interface position $h(\mathcal{X},\tau)$ is given by

$$\frac{\partial h}{\partial \tau} + \frac{\partial}{\partial \mathcal{X}} \int_{\beta}^{h(\mathcal{X})} u_1^{(0)} dy = 0, \tag{A.1}$$

and the integral occurring in the above equation is obtained as

$$\begin{aligned}\int_{\beta}^{h(\mathcal{X})} u_1^{(0)}\, dy = -\frac{(h^2-1)^2}{f_6(h)}\big[& f_1(h)\big(8+5qf_2(h)\big)q' \\ & + \big(4(h^2-1) - 4qf_3(h) + q^2 f_4(h)\big)h' \\ & + f_5(h)h'''\big],\end{aligned} \tag{A.2}$$

where the functional dependence of the variables q and h on $\mathcal{X}$ has been suppressed for brevity, and primes denote derivatives with respect to $\mathcal{X}$: $h' = \partial h/\partial \mathcal{X}$, $c' = \partial c/\partial \mathcal{X}$. The functions $f_1(h),\ldots,f_6(h)$ are given by

$$f_1(h) = (-3 - h + 3h^2 + h^3), \tag{A.3}$$

$$f_2(h) = (1 + 6h + h^2), \tag{A.4}$$

$$f_3(h) = (-7 - 18h + h^2), \tag{A.5}$$

$$f_4(h) = (-13 + 36h + 130h^2 + 36h^3 + 3h^4), \tag{A.6}$$

$$f_5(h) = 2(3+h)^3(h^2-1), \tag{A.7}$$

$$f_6(h) = 6(3+h)^2(33 + 12h + 6h^2 + 12h^3 + h^4). \tag{A.8}$$

The long-wave evolution equation the interfacial charge $q(\mathcal{X},\tau)$ is given by

$$\frac{\partial q}{\partial \tau} + \frac{\partial (u_1^{(0)} q)}{\partial \mathcal{X}} = S_1^{(0)} \frac{\partial \psi_1}{\partial y} - S_2^{(0)} \frac{\partial \psi_2}{\partial y}, \tag{A.9}$$

where all the quantities are to be evaluated at the interface $y = h(\mathcal{X})$. The tangential velocity of the fluid at the interface is given by

$$\begin{aligned}u_1^{(0)}[h] = \frac{-3}{(3+h)f_6}\big[& (h^2-1)\big(f_1(4f_2+qf_7)q' \\ & + 2(f_8 + 8qf_9 + q^2 f_{10})h' + (3+h^3)f_8 h'''\big)\big],\end{aligned} \tag{A.10}$$

where the variables $f_7,\ldots,f_{10}$ are functions of h, given by

$$f_7(h) = 19 + 36h + 98h^2 + 36h^3 + 3h^4, \tag{A.11}$$

$$f_8(h) = -1 - 6h + 6h^3 + h^4, \tag{A.12}$$

$$f_9(h) = 5 + 9h + 15h^2 + 3h^3, \tag{A.13}$$

$$\begin{aligned}f_{10}(h) = {} & 5 + 42h + 111h^2 + 228h^3 + 107h^4 \\ & + 18h^5 + h^6.\end{aligned} \tag{A.14}$$

Finally, the derivatives of the potentials occurring in (A.9) are given by

$$\left(\frac{\partial \psi_1}{\partial y}\right)_{h(\mathcal{X})} = -\frac{1 + q(1+h)}{3+h}, \tag{A.15}$$

$$\left(\frac{\partial \psi_2}{\partial y}\right)_{h(\mathcal{X})} = \frac{-2 + q - qh}{3+h}. \tag{A.16}$$

This completes the specification of the evolution equations.

Appendix B. List of symbols

μ_i	Viscosity of the fluid i
σ_i	Conductivity of the fluid i
ϵ_i	Dielectric constant of the fluid i
ψ_i	Potential in fluid i
$\mathbf{E}_i$	Electric field in fluid i
$S_i^{(0)}$	Scaled nondimensional conductivity in fluid i
ψ_b	Dimensional potential difference between the two plates
H	Thickness of fluid 2 in the unperturbed state
β	Ratio of thickness of fluid 1 to fluid 2
μ_r	Ratio of viscosities $= \mu_2/\mu_1$
γ	Interfacial tension between the two fluids
$h(x)$	Position of the interface between fluids 1 and 2
u_i	x-component velocity in fluid i
v_i	y-component velocity in fluid i
k	Wavenumber of perturbations
s	Growth rate of perturbations

References

[1] G.I. Taylor, A.D. McEwan, J. Fluid Mech. 22 (1965) 1–15.
[2] J.R. Melcher, C.V. Smith, Phys. Fluids 12 (1969) 778–790.
[3] D.A. Saville, Annu. Rev. Fluid Mech. 29 (1997) 27–64.
[4] E. Schaffer, T. Thurn-Albrechet, T.P. Russel, U. Steiner, Nature 403 (2000) 874–877.
[5] E. Schaffer, T. Thurn-Albrechet, T.P. Russel, U. Steiner, Eur. Phys. Lett. 53 (2001) 518–523.
[6] Z. Lin, T. Kerle, S.M. Baker, D.A. Hoagland, E. Schaffer, U. Steiner, T.P. Russel, J. Chem. Phys. 114 (2001) 2377–2381.
[7] Z. Lin, T. Kerle, T.P. Russel, E. Schaffer, U. Steiner, Macromolecules 35 (2002) 3971–3976.
[8] M.D. Morariu, N.E. Voicu, E. Schaffer, Z. Lin, T.P. Russell, U. Steiner, Nat. Mater. 2 (2003) 48–52.
[9] S.Y. Chou, L. Zhuang, J. Vac. Sci. Technol. B 17 (1999) 3197–3202.
[10] S.Y. Chou, L. Zhuang, L. Guo, Appl. Phys. Lett. 75 (1999) 1004–1006.
[11] S. Herminghaus, Phys. Rev. Lett. 83 (1999) 2539–2542.
[12] L.F. Pease III, W.B. Russel, J. Non-Newtonian Fluid Mech. 102 (2002) 233–250.